Available online at www.sciencedirect.com
SCIENCE DIRECT
International Journal of Heat and Mass Transfer 49 (2006) 3121–3129
International Journal of HEAT and MASS TRANSFER
www.elsevier.com/locate/ijhmt

Interfacial condensation for countercurrent steam–water stratified wavy flow in a horizontal circular pipe

Kyung-Won Lee [a], In-Cheol Chu [b], Seon-Oh Yu [c], Hee Cheon No [a,*]

[a] Department of Nuclear and Quantum Engineering, Korea Advanced Institute of Science and Technology, 373-1 Guseong, Yuseong, Daejeon 305-701, Republic of Korea
[b] Thermal Hydraulic Safety Research Division, Korea Atomic Energy Research Institute, P.O. Box 105, Yuseong, Daejeon 305-600, Republic of Korea
[c] Korea Institute of Nuclear Safety, 19 Guseong, Yuseong, Daejeon 305-338, Republic of Korea

Received 26 August 2005; received in revised form 10 February 2006
Available online 27 April 2006

Abstract

We experimentally investigate the interfacial condensation heat transfer for a steam–water countercurrent stratified flow in a horizontal pipe. In contrast to the previous work of Chu et al. [I.C. Chu, S.O. Yu, M.H. Chun, Interfacial condensation heat transfer for countercurrent steam–water stratified flow in a circular pipe. J. Korean Nucl. Soc. 32 (2) (2000) 142–156] that investigated only the interfacial condensation heat transfer in a stratified smooth flow in a horizontal pipe, this work investigates the steam–water stratified wavy flow. A total of 105 local interfacial condensation heat transfer coefficients for a wavy interface have been obtained. The parametric effects of the flow rates of steam and subcooled water and the degree of subcooling on condensation heat transfer were examined. The empirical Nusselt number correlation was developed on the basis of the bulk flow properties. This correlation agrees with the experimental data within ±32% with a RMS error of 16.2%. Its applicable ranges for a steam–water countercurrent stratified flow in a horizontal pipe are as follows: the ranges of Reynolds numbers are 4000–14000 for the water and 12000–23000 for the steam, and the Jakob numbers for the water are 43.5–180.

Keywords: Interfacial condensation; Stratified flow; Wavy flow; Horizontal pipe; Thick water layer; Thermal stratification

1. Introduction

The modeling of direct-contact condensation heat transfer in a steam–water stratified flow is important for the safety of nuclear reactor systems, especially for the condensation of steam on the emergency core cooling water in a cold leg during a postulated loss-of-coolant-accident sequence of a pressurized water reactor. The condensation-induced water hammer in a steam generator feedwater line is another well-known problem. Direct contact condensation heat transfer can also be encountered in a hot leg during a reflux condensation mode.

Over the past 30 years, a number of experimental studies [2–7] have investigated the interfacial condensation heat transfer in stratified concurrent and countercurrent steam–water flow. Some analytical works [8,9] have also investigated the heat transfer coefficient (HTC) at the steam–water interface. Table 1 shows details of the test section geometry and experimental conditions used by earlier workers. Most of the previous experimental studies (except for Ruile's work) used a wide rectangular channel and a very shallow water layer.

However, most piping in a nuclear power plant has a circular geometry rather than rectangular. Therefore, the flow geometry of existing works is not directly applicable to a nuclear piping system. When the cross-sectional area of a wide rectangular channel is the same as that of a circular pipe, the water layer of the circular channel is much thicker

* Corresponding author. Tel.: +82 42 869 3817; fax: +82 42 869 3810.
E-mail address: hcno@nsys.kaist.ac.kr (H.C. No).

0017-9310/$ - see front matter © 2006 Elsevier Ltd. All rights reserved.
doi:10.1016/j.ijheatmasstransfer.2006.02.017

Nomenclature

A_p	cross-sectional flow area (m^2)
C_p	specific heat (J/kg °C)
D	inside diameter of circular channel (m)
D_h	equivalent hydraulic diameter (m)
g	gravitational acceleration (m/s^2)
h	local heat transfer coefficient, HTC (W/m^2 °C)
i	specific enthalpy (J/kg)
i_{fg}	latent heat of condensation (J/kg)
j_k	superficial velocity of phase k (m/s)
Ja	Jakob number
k	conductivity (W/m °C)
L	channel length (m)
Nu	Nusselt number
Pr	Prandtl number
q''_{atm}	heat flux to the atmosphere due to steam condensation at the wall (W/m^2)
q''_i	heat flux to the water layer due to steam condensation at the interface (W/m^2)
Re	Reynolds number
S	wall perimeter (m)
S_i	interface perimeter (m)
T	temperature (°C)
T_f	bulk water temperature (°C)
V	velocity (m/s)
W	mass flow rate (kg/s)
x	axial distance from the water inlet (m)
y	vertical distance from the bottom of the pipe (m)
z	horizontal cross-stream distance from the center line of the pipe (m)

Greek symbols

δ	water layer thickness (m)
θ	inclination angle (degree; °)
μ	viscosity (Ns/m^2)
ρ	density (kg/m^3)

Subscripts

f	water; water side
g	saturated steam; steam side
i	interface
in	inlet of water or steam
sat	saturated value
m	averaged value in z-direction
c	value along the center line

Superscript

—	average value

than that of the wide rectangular channel for the given flow rates of steam and water. In particular, when the thickness of the water layer is increased, there is a change in the characteristics of the heat, mass and momentum transport, such as the turbulent intensity profile and the efficiency of turbulent mixing in the water layer, which are dominant in the interfacial condensation heat transfer. Therefore, the difference in the flow geometry may change the overall interfacial condensation heat transfer characteristics. According to Ruile's study [7], a thick water layer (about 40 mm) preventes full turbulent mixing and establishes thermal stratification. The limited turbulent mixing in the water layer, in turn, reduces the convective heat transfer mechanism as well as the interfacial heat and mass transfer property.

The main objective of this study is to experimentally investigate the condensation heat transfer of saturated steam in direct contact with the wavy countercurrent flow of a subcooled thick water layer in a nearly horizontal circular pipe. In contrast to a previous work of Chu et al. [1] that investigated only the steam–water tratified smooth flow, in this work, we investigate the steam–water stratified wavy flow. This work also aims to determine the paramet-

Table 1
Comparison of test section geometry and experimental conditions

Authors and references	Test section geometry and test condition				
	Channel geometry (inclination)	Dimension (cm) (width × height)	Flow direction	Water level (cm)	Interface conditions
Chu et al. [1]	Circular (horizontal)	ID = 8.4	Countercurrent	1.8–3.2	Smooth
Linehan et al. [2]	Rectangular (horizontal)	15 × 1.9	Cocurrent	0.05–0.15	Wavy
Segev et al. [3]	Rectangular (17°, 45°)	15.2 × (5.1–15.2)	Countercurrent	–	Wavy
Lim et al. [4]	Rectangular (horizontal)	30.48 × 6.35	Cocurrent	0.95–2.22 (inlet) 0.5–1.0 (downstream)	Smooth/wavy
Kim et al. [5]	Rectangular (4°, 30°, 33°, 87°)	38 × (7.5, 3.8)	Countercurrent	0.1 – 0.7	Smooth/Wavy
Rulie [6]	Rectangular (horizontal)	7.9 × 6.6	Cocurrent and Countercurrent	~4	Smooth (cocurrent) Wavy (countercurrent)
Choi et al. [7]	Rectangular (2.1°, 5°)	12 × 4	Cocurrent	0.1–0.3	Wavy
Present work	Circular (horizontal)	ID = 8.4	Countercurrent	1.3–2.8	Wavy

ric effects of a thick water layer, the steam and water flow rates, and the water subcooling on the interfacial condensation heat transfer.

2. Experiments

2.1. Experimental apparatus

Fig. 1 shows a schematic of the experimental apparatus. The test facility is designed and constructed such that the condensation rates of the steam along the circular channel can be measured while the saturated steam and subcooled water flow in the opposite direction. The test apparatus consists of a test section, a steam and water supply system, associated piping, and a data acquisition system.

The test section is slightly inclined (about 0.2° from the water inlet) and consists of several transparent tempered glass pipes that were connected in series by flanges. A traversable pitot tube with a outer diameter of 1.6 mm and a thermocouple with a outer diameter of 0.5 mm are installed at the bottom of each flange located at five different axial positions. Fig. 2 shows a schematic of the test section. The total length of the horizontal channel is 2.0 m and the inside diameter is 0.084 m. The test section used in this study has the same inside diameter as that used in Chu et al.'s experiment [1]. However, we amended the test section and instrumentation to enable a more suitable investigation for the interfacial condensation heat transfer under wavy interface conditions. Due to condensation, the steam flow rate decreases as the steam flows through the test section. As a result, the wavy interface cannot be maintained downstream of the steam flow. In our experiemnt, therefore, five pitot tubes and thermocouples are placed in the region close to the steam inlet.

The steam, which is supplied by a 200 kW electric steam boiler, passes through a steam–water separator. Before the steam flows into the test channel, the steam flow rate and thermal property are measured. The steam–water separator is used to ensure the supply of dry saturated steam or slightly superheated steam. The volumetric steam flow rate at the inlet of the test section is measured by a vortex flowmeter. The density of the steam, on the other hand, is evaluated on the basis of the temperature and pressure, which are measured by a thermocouple and an absolute pressure transmitter. A water surge tank (1.0 m^3) is used to provide a steady flow rate as well as the constant temperature of the water. The volumetric flow rate of the water that flows into the test section is measured by a turbine flowmeter. The vortex flowmeter was calibrated at the Korea Research Institute of Standards and Science. The turbined flowmeter was calibrated at Omega Eng. Inc., and the pitot tubes were calibrated using a specially designed calibration loop.

2.2. Test parameters and test procedure

The controllable test parameters were, firstly, the inlet flow rates of the water and steam and, secondly, the subcooling of the inlet water. Table 2 summarizes the test conditions. The range of Reynolds numbers was 4000–14 000 for the water (Re_f) and 12 000–23 000 for the steam (Re_g). The Jakob number (Ja) for the water varied from 43.5–180.

The definitions of dimensionless numbers are as follows:

$$
\begin{aligned}
Nu &= \frac{hD_{h,f}}{k_f}, \\
Re_f &= \frac{\rho_f V_f D_{h,f}}{\mu_f}, \quad Re_g = \frac{\rho_g V_g D_{h,g}}{\mu_g}, \\
Ja &= \frac{\rho_f C_{p,f}(T_g - T_f)}{\rho_g i_{fg}}, \\
D_{h,f} &= \frac{4A_{p,f}}{S_i + S_f}, \quad D_{h,g} = \frac{4A_{p,g}}{S_i + S_g},
\end{aligned}
\tag{1}
$$

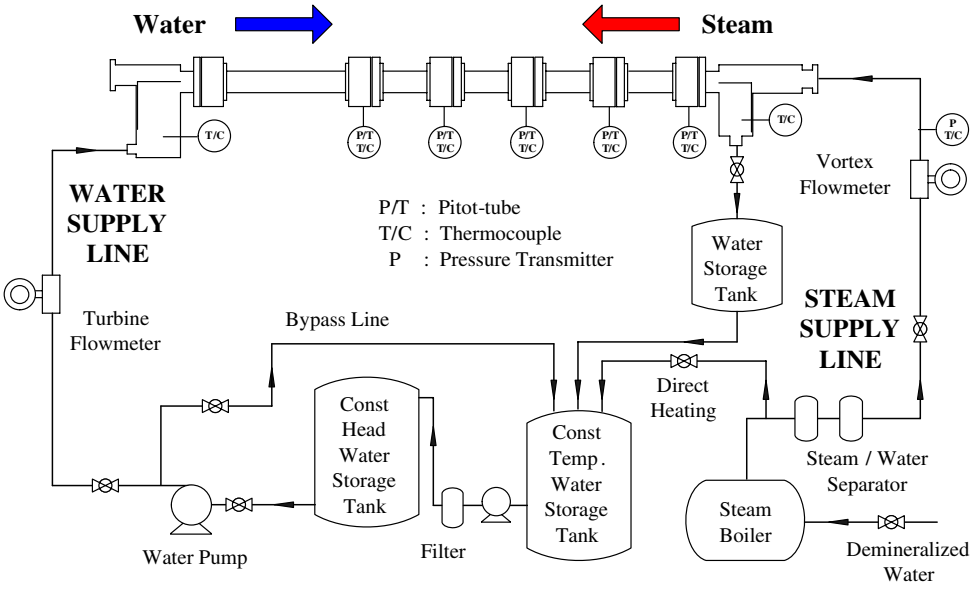

Fig. 1. Schematic of the experimental apparatus.

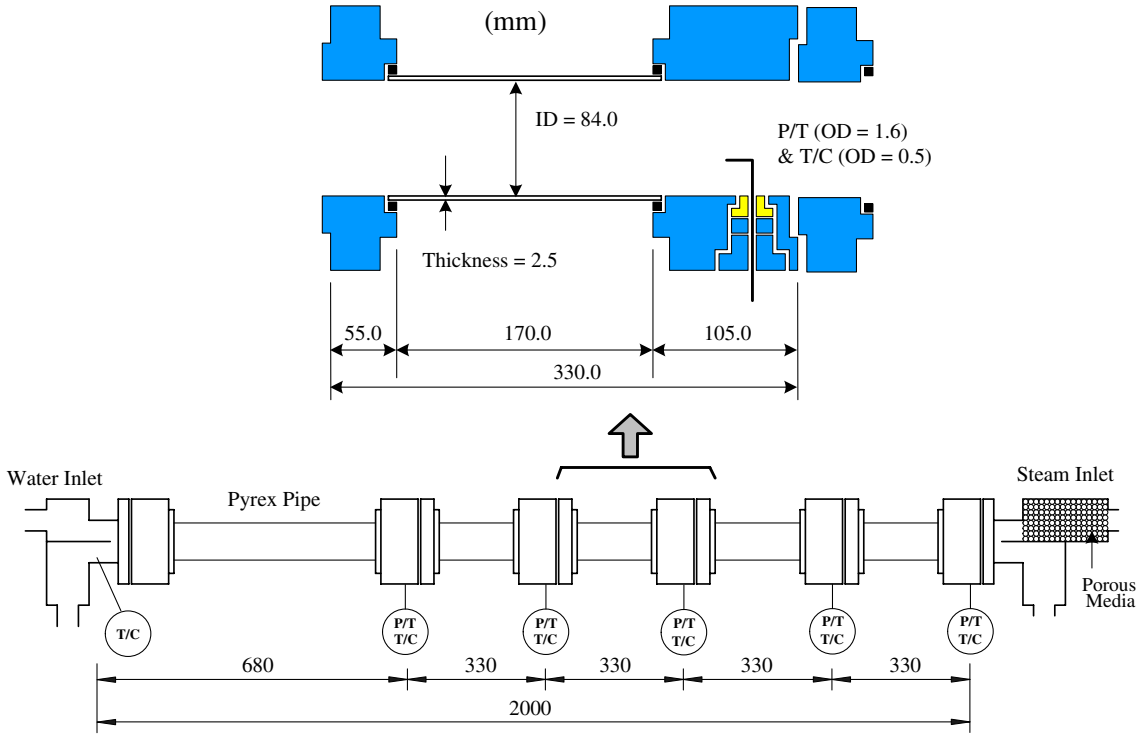

Fig. 2. Dimensions of the test section for the wavy interface experiments.

Table 2
Test matrix of the present experiments

$T_{f,in}$ (°C)	$T_{g,in}$ (°C)	$W_{f,in}$ (kg/s)	$W_{g,in}$ (kg/s)	Re_f	Re_g	Ja	Number of data
25	100	0.08–0.22 (5 cases)	0.013–0.019 (6 cases)	4000–10000	12000–19000	77.9–180	41
45	100	0.08–0.22 (5 cases)	0.015–0.018 (6 cases)	4000–13000	14000–17000	52.2–131	31
55	100	0.08–0.22 (5 cases)	0.015–0.02 (6 cases)	4000–14000	17000–23000	43.5–99.1	33
	Total number of data						105

where Nu is the Nusselt number, h is the interfacial condensation HTC, D_h is the hydraulic diameter, A_p is the cross-sectional flow area, and S is the perimeter. The subscript i denote the steam–water interface and the subscripts f and g denote the liquid phase and gas phase, respectively. In using these equations, we evaluate all liquid properties at the bulk temperature of liquid layer.

The condensation rate of the steam at the steam–water interface was deduced from the increase rate of the bulk water temperature due to steam condensation. To evaluate the bulk water temperature along the flow stream, measurements were taken of the vertical velocity distributions of the water layer and the bulk water temperature at five axial positions along the test section.

A brief outline of the test procedure is as follows. First, the water temperature in the surge tank is brought to a predetermined value for each test run. The inlet flow rates of the water and steam are then set at desired values with the aid of a pump rpm controller and valve opening adjustment, respectively. Second, when the desired steam and water flow rates reach steady conditions, the radial distributions of the temperature and the velocity of the water at five different axial position along the test section are simultaneously measured by traversing the pitot tubes and thermocouples from the bottom of the pipe to the steam–water interface. The pitot tubes and thermocouples are attached to a travering system with a mounted digital vernier caliper; and they are attached in such a way that both the pitot tubes and the thermocouples could be raised vertically by an increment of 1.0 mm. All measurements except the water film thickness, are recorded by the data acquisition system. Third, the water layer thickness (δ) at each axial position is determined by both the visual observation and the degree of water subcooling measured by the thermocouples.

3. Method of analysis

Fig. 3 shows the control volume describing the heat transfer process in a countercurrent steam–water stratified flow in a horizontal pipe. An outline of the procedure to obtain the interfacial condensation HTC is as follows:

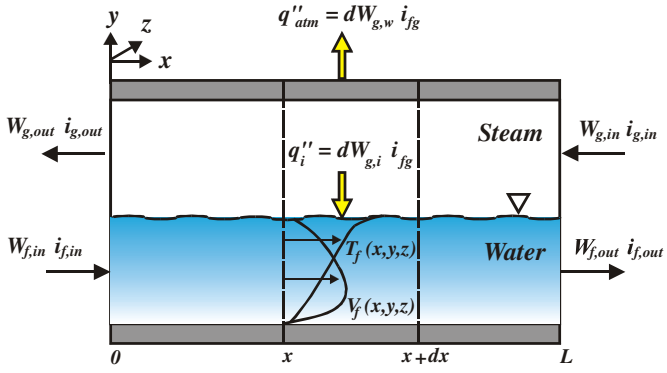

Fig. 3. Control volume of the countercurrent steam–water stratified flow.

(I) Based on the mass and energy balance, the local interfacial condensation HTC at any location x from the water inlet can be expressed as

$$h(x) = \frac{i_{fg}}{S_i(T_g - T_f(x))}\frac{dW_f}{dx}, \tag{2}$$

where W_f denotes the mass flow rate of water. Therefore, the interfacial condensation HTC can be deduced from the increase rate of local water flow rate along the axial direction of test section.

In the calculation of the condensation HTC, the bulk water temperature and the physical properties at each axial position were determined on the basis of the following assumptions:

(i) that the steam along the test section is at saturation condition
(ii) that the temperature of the water across the cross-section (in the z-direction in Fig. 3) at each vertical position is uniform
(iii) that the velocity of water across the cross-section (in the z-direction in Fig. 3) at each vertical position has the 1/7 power velocity profile.

Actually, the temperature drop between steam inlet and outlet was less than 1 °C and the experimental results of Chu et al. [1] for the smooth interface showed the the water temperature for different levels of water layer did not vary significantly in the z-direction. Additional analyses also showed that the velocity profile in the z-direction has a negligible effect on bulk water temperature.

(II) Using the relations of the mass and energy conservation for the control volume shown in Fig. 3, the local mass flow rate of water, $W_f(x)$, can be expressed as

$$W_f(x) = \frac{W_{f,in}(i_g - i_{f,in}) + \int_0^x q''_{atm} S_g dx}{i_g - i_f(x)}, \tag{3}$$

where q''_{atm} is the heat flux to the atmosphere through the wall of the steam side and S_g is the wall perimeter of the steam side. The steam condensation rates at the wall of the test section and the steam reservoir were evaluated by directly measuring the heat flux to the atmosphere using a microfoil heat flux sensor with an accuracy of ±3%. The results showed that the condensation rate at the wall could be neglected when calculating the interfacial condensation HTC. Hence, the term of heat flux to the atmosphere is ignored.

(III) In Eq. (3), the local mass flow rate of the water can be evaluated from the bulk water temperature. The bulk water temperature at any x is defined as follows

$$T_f(x) = \frac{\int \rho_f(x,y,z) T_f(x,y,z) V_f(x,y,z) dy dz}{\int \rho_f(x,y,z) V_f(x,y,z) dy dz}. \tag{4}$$

Eq. (4) can be approximated by the following equation and, as shown in Fig. 4, $T_f(x)$ can be evaluated by integrating the measured local temperature and velocity profiles over the area of the water layer divided into several rectangular cells;

$$T_f(x) = \frac{\sum_j^n \rho_{f,m}(y_j) T_{f,m}(y_j) V_{f,m}(y_j) S_i(y_j) \Delta y_j}{\sum_j^n \rho_{f,m}(y_j) V_{f,m}(y_j) S_i(y_j) \Delta y_j z}, \tag{5}$$

where the subscript m refers to the value averaged in the z-direction for each rectangular cell. Using assumptions (ii) and (iii), Eq. (5) can be further simplifed as follows:

$$T_f(x) \cong \frac{\sum_j^n a(y_j) \rho_{f,c}(y_j) T_{f,c}(y_j) V_{f,c}(y_j) S_i(y_j) \Delta y_j}{\sum_j^n a(y_j) \rho_{f,c}(y_j) V_{f,c}(y_j) S_i(y_j) \Delta y_j z}, \tag{6}$$

where the subscript c refers to the value measured at central point of each rectangular. In Eq. (6), $a(y_j)$, which is the ratio between the average and the center line velocity at each vertical position of y_j, is defined by

$$a(y) = \frac{V_{f,m}(y)}{V_{f,c}(y)} = \frac{\int_0^{\frac{S_i}{2}} \left[\frac{R - \sqrt{(R-y)^2 + z^2}}{y}\right]^{1/7} dz}{\int_0^{\frac{S_i}{2}} dz}. \tag{7}$$

The value of $a(y)$ for each vertical position of y can be obtained by numerical integration, and the following expression can be obtained by a fourth order polynomial curve fitting:

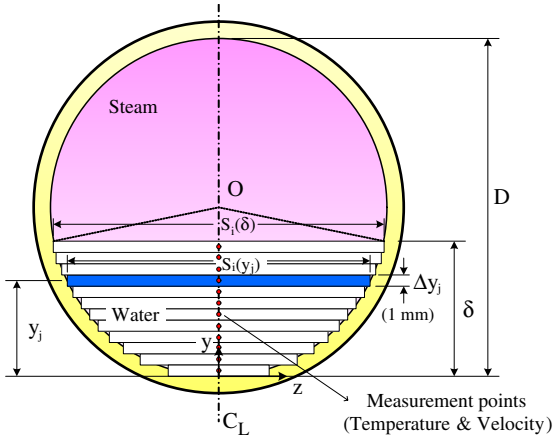

Fig. 4. Nodalization of the water layer into rectangular cells.

$$a(y) = 0.922 - 0.016(y/R) - 0.035(y/R)^2 + 0.042(y/R)^3 - 0.038(y/R)^4. \quad (8)$$

When the laminar velocity profile is assumed, $a(y)$ has a constant value of 2/3, regardless of the value of y. However, the change in $a(y)$ depending on the turbulent or laminar velocity profile has a negligible effect on the bulk water temperature. Because of the difficulty of measuring the velocity near the steam–water interface, the velocity of this region is evaluated by extrapolating the measured velocity profile and assuming there is no slip at the interface.

4. Results and discussion

A total of 105 local interfacial condensation HTCs were obtained for the wavy interface conditions, for various combinations of the following initial conditions: the inlet water flow rate, inlet steam flow rate, and degree of water subcooling.

4.1. Flow regime

Fig. 5 shows the experimental data plotted in the Mandhane's flow pattern map [10]. Visual observations showed that the transition from the stratified smooth to the wavy flow occurred when the local steam superficial velocity was greater than about 2.5 m/s for the range of the water superficial velocity of 0.01–0.05 m/s. The gas superficial velocities required for the transition from the smooth to the wavy interface are lower in steam–water experiments than in air–water experiments, because the interfacial shear stress in the presence of condensation is augmented by the mass transfer [2].

The water layer thicknesses were from 0.013 m to 0.028 m. The ratio of the water layer thickness to pipe diameter varied from 0.155 to 0.333, which was much greater than the ratio obtained in the previous works for a wide rectangular channel. In our experiment, a three-dimensional pebble wave was dominant.

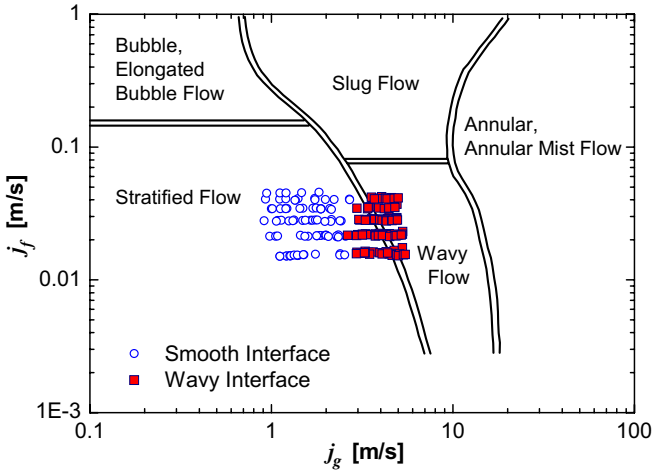

Fig. 5. Experimental data plotted in the Mandhane's flow pattern map.

4.2. Profiles of the local temperature and velocity of the water

Figs. 6 and 7 show typical profiles of the local water temperature and the local water velocity measured at 1.67 m downstream from the water inlet for three inlet water temperatures of 25 °C, 45 °C, and 55 °C. To evaluate the effect of the steam–water interface condition on the heat transfer characteristics, the results of Chu et al. [1] for the smooth interface, which were measured at 1.6 m down stream from the water inlet, are also presented.

Fig. 6 shows that, for the smooth interface conditions, the local temperature of the water layer close to the bottom (i.e., $y/\delta < 0.6$) is slightly higher than the inlet water temperature and remains fairly constant. The figure also shows that in the region of the higher water layer (i.e., $y/\delta > 0.8$) the temperature of the water layer tends to rise sharply to the saturation temperature. For the wavy interface condi-

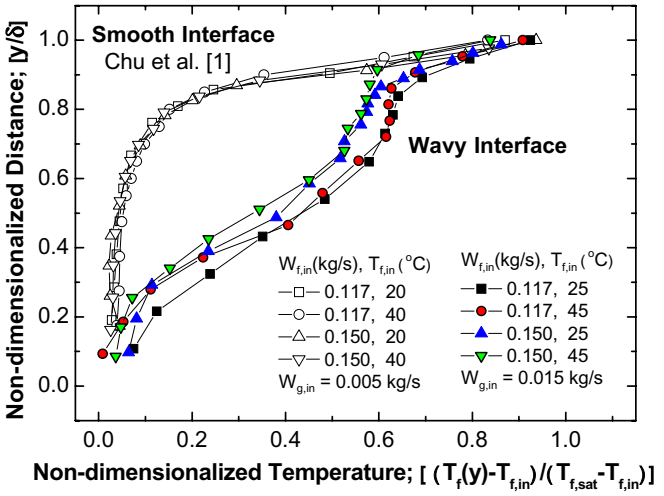

Fig. 6. Non-dimensionalized local temperature profiles of the water layer.

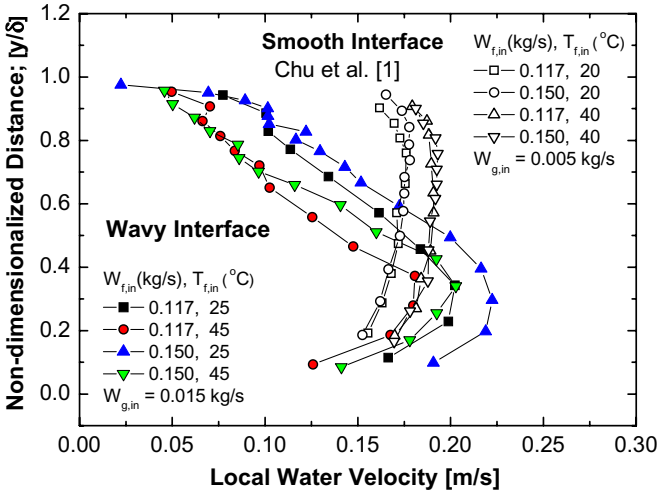

Fig. 7. Local velocity profiles of the water layer.

tions, as opposed to the smooth interface conditions, the local temperature of the water layer in the region of $y/\delta < 0.6$ does not remain constant but rises more or less gradually. In the region close to the interface, however, the temperature profile of the wavy interface shows a similar trend to the smooth interface conditions.

Fig. 7 shows that, for the smooth interface conditions, the local velocity of the water layer reaches a high velocity region at around $y/\delta = 0.5$ and remains more or less constant. For the wavy interface conditions, however, the local velocity of water layer reaches a maximum value at around $y/\delta = 0.3$, and significantly slows down as it moves toward the interface due to the enhanced shear stress of the countercurrent steam flow. The local water velocity at steam–water interface is nearly zero.

If there were full turbulent thermal mixing in the water layer, the temperature profile should be almost uniform. The curves in Fig. 6 imply that the thick water layer (0.018–0.032 m for the smooth interfaces and 0.013–0.028 m for the wavy interfaces) in the circular channel prevents the water layer from inducing full turbulent thermal mixing and forms thermal stratification in the water layer, especially for the smooth interface conditions. That is, the turbulence generated by the interfacial shear does not propagate into the lower region of the water layer, and effective turbulent thermal mixing is restricted within the upper region of the water layer close to the steam–water interface. Therefore, the thermal resistance of the water layer to the interfacial condensation heat transfer was fairly large.

However, the turbulence generated by the interfacial shear stress can be propagated into lower region of water layer more efficiently for the wavy interface conditions than for the smooth interface conditions, as shown in Figs. 6 and 7.

Fig. 8 shows how the bulk temperature of the water increases along the water flow stream for both smooth and wavy interface conditions. As expected, the increase rate of the bulk water temperature for the wavy interface conditions is much larger than that for the smooth interface conditions. This phenomenon occurs because for the wavy interface conditions there is a greater convective heat transfer due to the mixing in the water layer. Moreover, the bulk water temperature increases almost linearly with respect to the distance from the water inlet. This result implies that the gradient of the water mass flow rate or, equivalently, the steam mass flow rate in Eq. (2) can be approximated as follows

$$\frac{dW_f(x)}{dx} = \frac{W_f(x+1) - W_f(x-1)}{2\Delta x}, \tag{9}$$

where Δx is the distance between two adjacent measurement positions, and $x+1$ and $x-1$ refer to the next and the previous axial measurement positions of x, respectively.

4.3. Effects of the flow rates of the steam and water and the water subcooling

In this study, the local interfacial condensation HTCs varied from 1.9 to 5.1 kW/m^2 °C. In Figs. 9 and 10, the local Nusselt number versus the local steam (and water) Reynolds number are shown for different ranges of the water (and steam) Reynolds numbers and the inlet water temperatures. The results of Chu et al. [1] are presented to investigate the influence of the interface conditions.

The effects of the water and steam flow rates on the interfacial condensation HTC for the wavy interface conditions can be deduced from Figs. 9 and 10. That is, for a given water Reynolds number (or water flow rate), the Nusselt number (or h) increases as the steam Reynolds number (or steam flow rate) increases. In addition, for a given steam Reynolds number, the Nusselt number increases when the water Reynolds number increases. These results are consistent with the experimental results of Chu et al. [1] for the smooth interface conditions.

In the absence of a complete turbulent mixing motion, the interface shear enhances the convection. This enhancement explains how the condensation HTC (or equivalently,

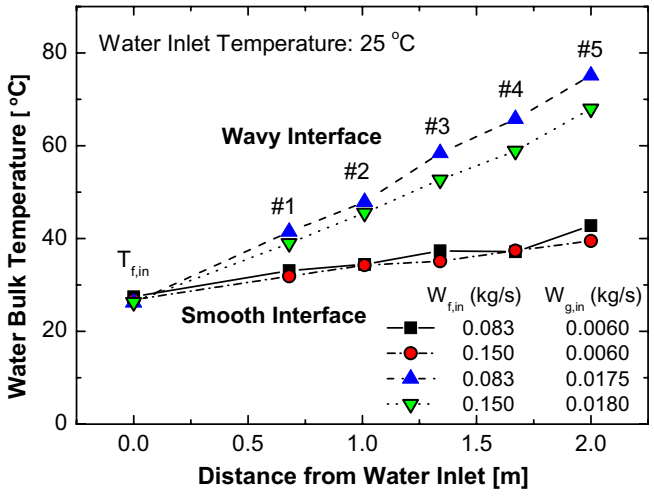

Fig. 8. Increase rate of the bulk water temperature along the flow stream.

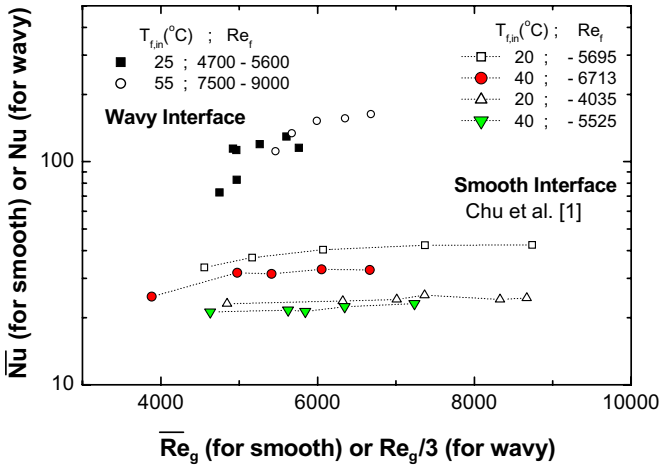

Fig. 9. Effects of the steam flow rate on the interfacial condensation heat transfer.

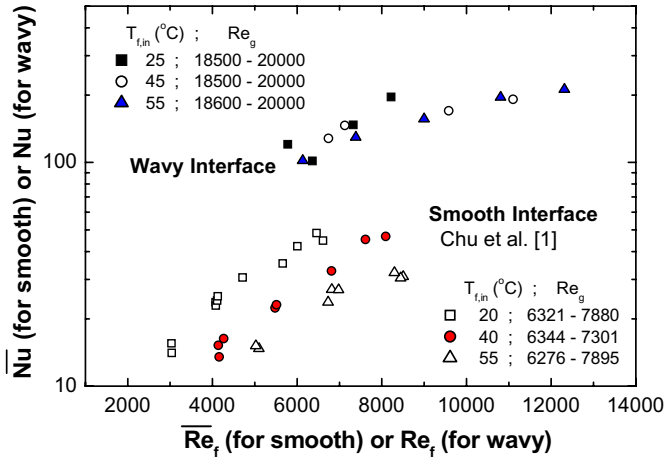

Fig. 10. Effect of the subcooling of water and the water flow rate on the interfacial condensation heat transfer.

the Nusselt number) increases with the higher steam Reynolds numbers. The increase in the condensation HTC with the water flow rate, however, is mainly due to the following two factors: first, at higher water flow rates, the water temperature increases slowly from the inlet value and the temperature difference between the water layer and the steam consequently remains relatively large; and, second, the increase in the water flow rate may also increase the initial turbulence in the water and therefore increase the condensation heat transfer.

As can be seen in Figs. 9 and 10, for the smooth interfaces conditions, the subcooling of water had definite effect on the HTC: the HTC increases as the bulk water temperature decreases (that is, as the subcooling of water increases) for a given steam and water Reynolds numbers. However, for the wavy interface conditions, it is difficult to evaluate directly the effect of the subcooling of water on the HTC due to the lack of experimental data.

4.4. Empirical correlation for the interfacial condensation HTC

To correlate the 105 experimental data obtained for the wavy flow in a nearly horizontal circular pipe, the local Nusselt number correlation was developed in terms of the water and steam Reynolds numbers and the water Jakob number using a least-square fit method as follows

$$Nu = 1.2 \times 10^{-7} Re_f^{0.59} Re_g^{1.2} Ja^{0.82} \quad (10)$$

(for a wavy interface, where $j_g > 2.5$ m/s).

The applicable ranges of Eq. (10) are

$$4000 < Re_f < 14000,$$

$$12000 < Re_g < 23000,$$

and

$$43.5 < Ja < 180.$$

All the dimensionless numbers included in Eq. (10) are defined in terms of the bulk flow properties shown in Eq. (1).

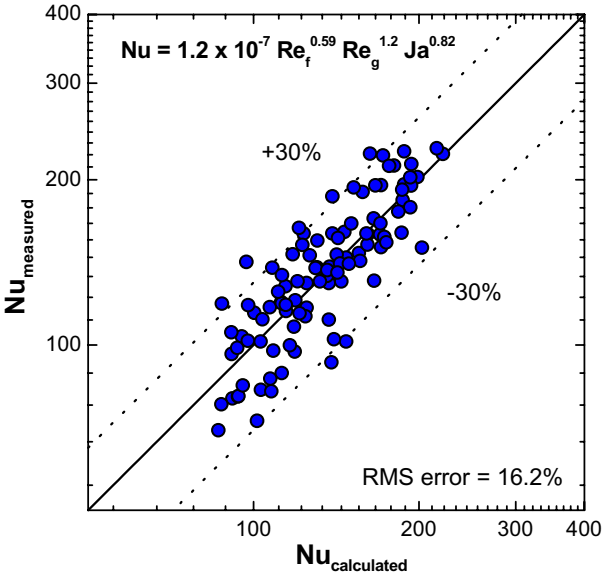

Fig. 11. Comparison of the measured Nusselt number with the calculated value.

The relatively large exponent of the steam Reynolds number, compared with the water Reynolds number, shows that the interfacial shear stress plays an important role in the condensation heat transfer for the wavy interface conditions. Fig. 11 compares the measured Nusselt number with the calculated values obtained from Eq. (10). The correlation agree with most of the data within ±32% (with a RMS error of 16.2%).

4.5. Uncertainty analysis

Based on Eq. (2), the uncertainty of the local HTCs is given by the root sum square of a bias contribution and a precision (random) contribution to the total uncertainty of the HTC. Each of these two contributions can be evaluated separately in terms of the sensitivity coefficients of the reduced data to measured parameters (partial differential terms) and the measurement errors of the parameters using the uncertainty propagation equation of Kline and McClintock [11]. The uncertainty analysis was performed in accordance with a 95% confidence level. Its detailed results are summarized in Table 3.

Table 3
Parameters and estimated uncertainties with a 95% confidence level

	Parameter	Bias limit	Precision limit
Independent parameter	δ (mm)	1.0	0.5
	$W_{f,in}$ (%)	0.5	0.5
	$V_{f,c}(x,y)$ (%)	5.0	0.5
	$T_{f,c}(x,y)$, T_g (°C)	2.2	0.1
Major dependent parameter	$T_f(x)$ (°C)	0.84–2.15	0.37–4.32
	$W_f(x)$ (%)	0.51–0.72	0.51–0.55
	h (%)	10.4–39.9	6.03–22.2
Mean of total uncertainty: h (%)		22.59	

5. Conclusions

We experimentally investigated the interfacial condensation heat transfer for countercurrent steam–water stratified wavy flow in a nearly horizontal circular pipe. The main conclusions are as follows.

- The condensation rates of saturated steam on a subcooled thick water layer (0.013–0.028 m) in a countercurrent horizontal circular channel were obtained by measuring the rate of increase in the bulk water temperature due to the condensation of steam, and the local interfacial condensation heat transfer coefficients were subsequently deduced.
- The measurements of local temperature and velocity profiles in the thick water layer show that the thermal resistance of the water layer is appreciably large because the turbulent thermal mixing generated by the interfacial shear does not propagate into the lower region of the water layer but is restricted to the upper region of the water layer near the steam–water interface. However, the turbulent thermal mixing can be propagated more efficiently into lower region of water layer for the wavy interface conditions than for the smooth interface conditions.
- The empirical local Nusselt number correlation for a wavy interface region was developed on the basis of the bulk flow properties. The correlation agree with most of the data within $\pm 32\%$.

References

[1] I.C. Chu, S.O. Yu, M.H. Chun, Interfacial condensation heat transfer for countercurrent steam–water stratified flow in a circular pipe, J. Korean Nucl. Soc. 32 (2) (2000) 142–156.
[2] J.H. Linehan, M. Petrick, M.M. El-Wakil, The condensation of a saturated vapor on a subcooled film during stratified flow, Chem. Eng. Progress Symp. Ser. 66 (102) (1970) 11–20.
[3] A. Segev, L.J. Flanigan, R.E. Kurth, R.P. Collier, Experimental study of countercurrent steam condensation, ASME J. Heat Transfer 103 (1981) 307–311.
[4] I.S. Lim, R.S. Tankin, M.C. Yuen, Condensation measurement of horizontal cocurrent steam/water flow, ASME J. Heat Transfer 106 (1984) 425–432.
[5] H.J. Kim, S.C. Lee, S.G. Bankoff, Heat transfer and interfacial drag in countercurrent steam–water stratified flow, Int. J. Multiphase Flow 11 (1985) 593–606.
[6] H. Ruile, Heat transfer by direct contact condensation in stratified two phase flow at high system pressure, Two-Phase Flow Model. Experiment., Rome, Italy (1995) 269–276.
[7] K.Y. Choi, H.J. Chung, H.C. NO, Direcet-contact condensation heat transfer model in RELAP5/MOD3.2 with/without noncondensable gases for horizontally stratified flow, Nucl. Eng. Des. 211 (2002) 139–151.
[8] A. Murata, E. Hihara, T. Saito, Prediction of heat transfer by direct contact condensation at a steam–subcooled water interface, Int. J. Heat Mass Transfer 35 (1) (1992) 101–109.
[9] J. Mikielewicz, A.M.A. Rageb, Simple theoretical approach to direct-contact condensation on subcooled liquid film, Int. J. Heat Mass Transfer 38 (3) (1995) 557–562.
[10] J.M. Mandhane, G.A. Gregory, K. Aziz, A flow pattern map for gas–liquid flow in horizontal pipes, Int. J. Multiphase Flow 1 (1974) 537–553.
[11] S.J. Kline, F.A. McClintock, Describing uncertainties in single-sample experiments, Mech. Eng. 75 (1953) 3–8.